UNIVERSITY OF BUCHAREST
FACULTY OF CHEMISTRY
DOCTORAL SCHOOL IN CHEMISTRY

PhD THESIS
ABSTRACT

COORDINATION POLYMERS BUILT WITH OLIGONUCLEAR NODES

PhD student: Teodora Mocanu

PhD Supervisor: Acad. Marius Andruh

Doctoral committee:

President: Prof. Dr. Camelia BALA

Supervisor: Acad. Marius ANDRUH

Official referents:

1. Acad. Cristian SILVESTRU, from Babeș-Bolyai University, Cluj-Napoca
2. Associate Prof. Augustin MĂDĂLAN, from University of Bucharest
3. Dr. Gabriela MARINESCU, from „Ilie Murgulescu" Institute of Physical Chemistry, Romanian Academy, Bucharest

2021

Table of content (according to the PhD thesis)

THEORETICAL PART

ORIGINAL CONTRIBUTIONS

Thesis topics

The subject of the PhD thesis with the title “Coordination polymers built with oligonuclear nodes” falls into the research fields of coordinative chemistry, metalosupramolecular and crystalline engineering. The thesis comprises four chapters and was structured in two parts: the theoretical part (chapter I) and the original part (chapters II, III and IV).

The theoretical part is composed of four subchapters in which the structures and properties of some compounds presented in the literature are discussed in terms of the topology of the three-dimensional networks. The analysis of solid state architecture from the perspective of concepts that topologically describe a network (connectivity and symmetry of the nodes, their orientation in three-dimensional space, circuits, the ratio of combining nodes in binodal networks, transitivity) allows the directionality of synthesis strategies towards the development of multifunctional materials. The design of extended polynuclear structures with interesting functionalities involves the selection of organic tectons or metal building blocks suitable for the construction of three-dimensional frameworks with predefined topology by correlating the properties of systems and the topological characteristics of networks (density, transitivity, hetero- or self-dual character, chirality). The replacement of topological nodes in the networks described by Wells with suitably symmetric organic ligands and metal ions with preference for certain stereochemistry in the “node and spacer” strategy proposed by Robson or oligonuclear clusters, in which metal ions are bridged by carboxylate groups, in the case of "reticular chemistry" developed by Yaghi allowed the rational construction of coordination polymers with predefined topologies.

A first objective of the PhD thesis is represented by the synthesis and characterization of extended polymetallic systems using different types of divergent ligands: organometallic molecules, spacer with tetrahedral or tetragonal symmetry. Another objective is the modulation of photoluminescent properties for molecular assemblies built with benzothiadiazole derivatives.

Directions of study:

Throughout the three chapters of the original part, the following directions of study were addressed:

- Synthesis and characterization of extended heterometallic structures by connecting metal nodes with organometallic spacers decorated with groups having potential donor atoms;
- Construction, based on co-crystallization processes, of supramolecular edifices by assembling supramolecular synthons generated by organometallic tectons;
- Design of new coordination polymers built with spacers grafted on square spirobifluorene platforms and characterization of photoluminescent properties;
- Synthesis and characterization of three-dimensional systems possessing different topologies where organic ligands play the role of tetrahedral nodes;
- Design of discrete units or coordination polymers constructed with bis-pyridyl-benzothiadiazole derivatives and modulation of the luminescent properties of the compounds obtained by the appropriate selection of metal nodes.

Original contributions

Chapter II addresses the first two directions of research and describes the systems obtained by using four organometallic molecules, which have pyridyl or nicotinato/isonicotinato fragments attached to metal centers (bis(4-pyridyl)mercury L^1, trimethylstibium(V)-bi(isonicotinate) L^2, triphenylbismuth(V)-bi(isonicotinate) L^3, triphenylbismuth(V) -bi(nicotinate) L^4 - scheme 1) as tectons in the assembly of heterometallic frameworks and supramolecular systems.

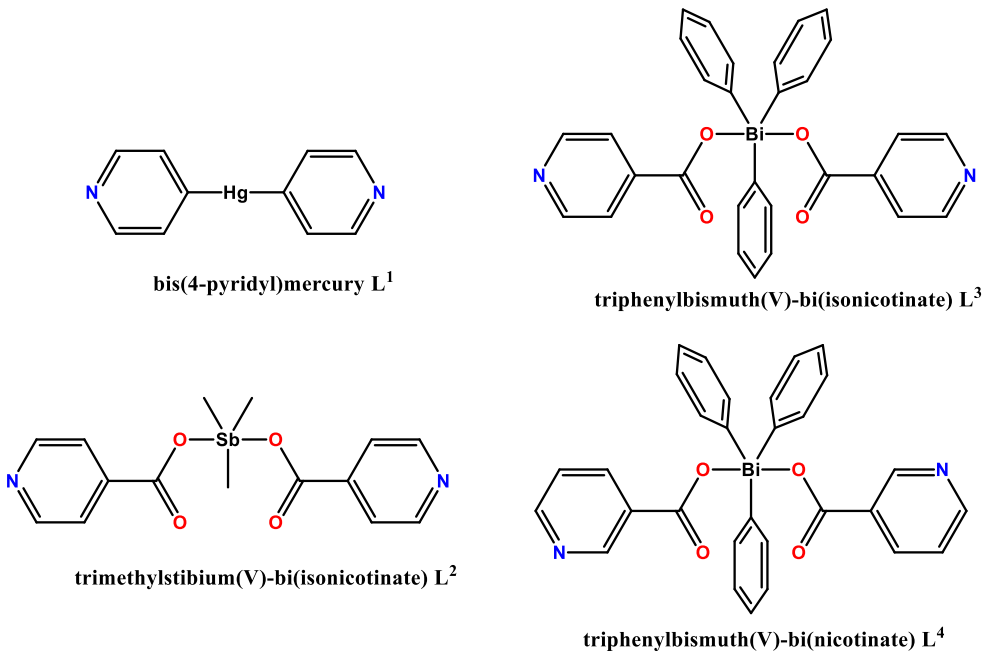

Scheme 1. Organometallic ligands used in this thesis.

Various molecular building blocks were used to test the coordination capacity of bis(4-pyridyl)mercury: mononuclear nodes; asymmetric bicompartmental complexes and Cu (II) alkoxido-binuclear nodes.

Following the reaction of bis(4-pyridyl)mercury with mononuclear nodes, one-dimensional chains are assembled. In compound **1**, the species {Mn(hfac)$_2$} are connected in linear chains by organometallic bridges that coordinate in the *trans* positions of the metal ions. The reaction between zinc(II) ions and bis(4-pyridyl)mercury, in the presence of 18-crown-6 ether, allows the formation of linear 1-D chains, which interact through hydrogen bonds with perchlorate anions and 18C6 molecules, resulting in three-dimensional supramolecular assemblies (figure 1).

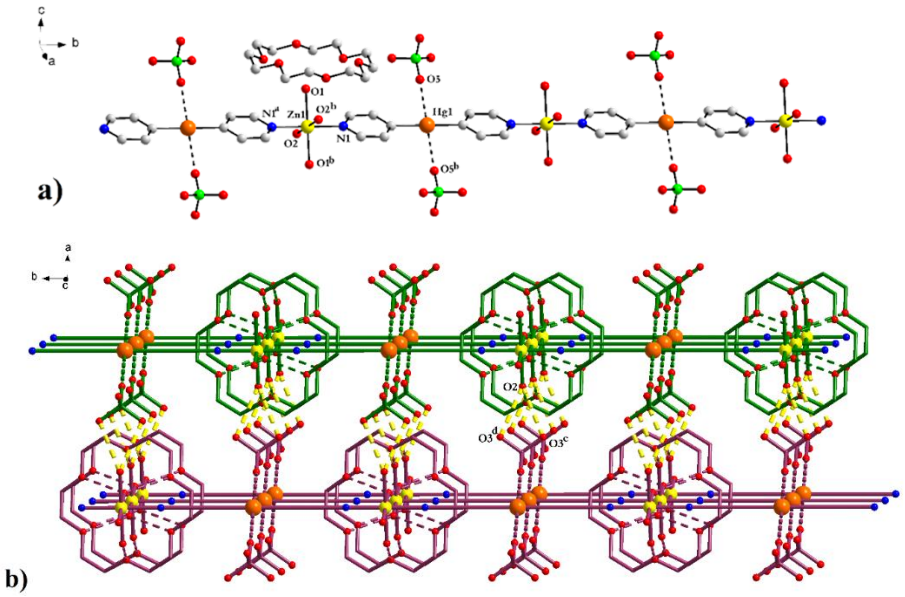

Figure 1. a) Perspective of a linear chain in the structure of the compound [Zn(H$_2$O)$_4$(L^1)](ClO$_4$)$_2$·18C6 **2**; b) Perspective of the three-dimensional network resulting from the establishment of bifurcated hydrogen bonds between perchlorate anions, water molecules coordinated to zinc (II) ions and crown ether molecules that function as a secondary sphere ligand. Symmetry operations: [a] = -*x*, -*y*, -*z*; [b] = -*x*, *y*, -*z*; [c] = *x*, -*y*, *z*; [d] = -0.5-*x*, -0.5+ *y*, -*z*; [e] = -0.5-*x*, 0.5-*y*, -*z*.

Compounds **3** and **4** show surprising structures and are the attempt of using asymmetric bicompartmental complexes as nodes in the construction of coordination polymers. The compound [Cu(valpn)(HL^1)][Cu(valpn)](CH$_3$COO)·H$_2$O **3** was obtained by reacting [Cu(valpn)], H$_2$valpn = Schiff base resulting from the condensation of 3-methoxysalicylaldehyde with 1,3-diaminopropane in a 2: 1 ratio, and bis(4-pyridyl)mercury, in the presence of a drop of concentrated acetic acid. Single-crystal X-ray diffraction data reveal the presence of two different components in the asymmetric unit: a neutral component

[Cu(valpn)], where the free O_2O_2' site hosts a water molecule, and a cationic component, $[Cu(valpn)(HL^1)]^+$, where monoprotonated organometallic tecton molecules coordinate through the nitrogen atom to the Cu(II) ion and interact through the Hg atom with the free O_2O_2' site in a neighboring unit, resulting in 1-D chains. The chains are interconnected by π–π stacking contacts between the phenyl rings in stair-like arrangements (figure 2a). In the case of compound **4**, where H_2valpa = Schiff base resulting from the condensation of 3-methoxysalicylaldehyde with 1,3-propanolamine in a 1: 1 ratio, the dinuclear complex $[Cu_2(valpa)_2]$ and L^1 molecules form a co-crystallization product $[Cu_2(valpa)_2]\cdot(L^1)$. At supramolecular level, the organic tecton molecules are associated in grids by Hg ⋯ N interactions (figure 2b).

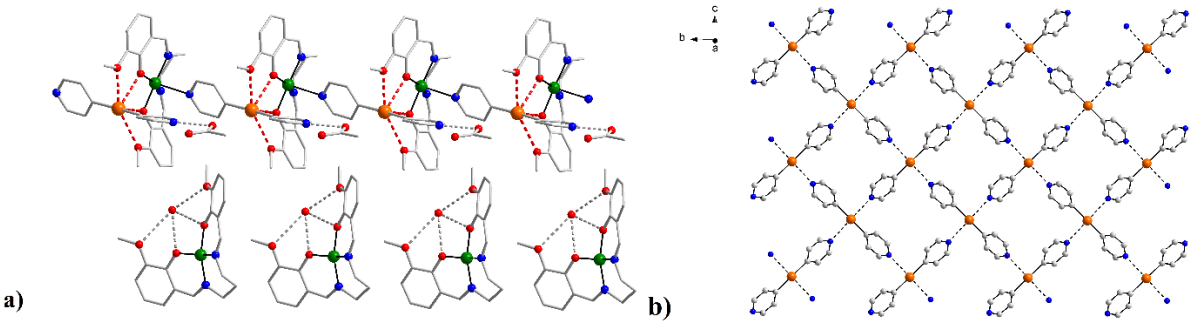

Figure 2. a) Crystal packing diagram for $[Cu(valpn)(HL^1)][Cu(valpn)](CH_3COO)\cdot H_2O$ **3**; b) View of a grid-like supramolecular layer constructed of L^1 molecules by Hg···N interactions in the compound $[Cu_2(valpa)_2]\cdot(L^1)$ **4**.

Attempting to obtain extended polynuclear systems, two low-denticity aminoalcohols were used: monoethanolamine (Hmea) and propanolamine (Hpa). The Cu(II) ions form, when reacting with bidentate aminoalcohols, alkoxido-binuclear species bearing two free positions for interacting with spacers and being suitable nodes for the generation of two-dimensional grid-like networks or three-dimensional frameworks. Three new compounds were synthesized: $[Cu(Hmea)_2(L^1)](ClO_4)_2\cdot 2(L^1)$ **5**, $[Cu_2(pa)_2(L^1)(ClO_4)_2]\cdot 0.5(L^1)\cdot H_2O$ **6**, $[Cu_2(pa)_2(L^1)_2](BF_4)_2$ **7**, using copper(II) salts, monoethanolamine or propanolamine and bis(4-pyridyl)mercury, in a 1: 4: 1 molar ratio and different solvents: methanol (for **6** and **7**) and a mixture of methanol and dichloromethane for **5**.

Compounds **5** and **6** are one-dimensional coordination polymers, with organometallic ligand molecules joining different metal building blocks (cationic mononuclear species $\{Cu(Hmea)_2\}^{2+}$ in **5**, binuclear nodes $\{Cu_2(pa)_2\}^{2+}$ in **6**, respectively) in linear chains. Compound **7** is a three-dimensional network. Perchlorate anions and uncoordinated organometallic tecton molecules participate in establishing non-covalent interactions (Hg···π,

Hg···O, hydrogen bonds) and connect the chains in three-dimensional supramolecular assemblies. In compound **5**, the two-dimensional layers, where uncoordinated L^1 molecules interact by a pyridyl group with the mercury atoms from the chains, through Hg ··· π contacts and by the other pyridyl fragment through hydrogen bonds with the NH_2 groups in the neighboring chains, are assembled in a 3-D network by Hg ··· O contacts established between perchlorate anions and bis(4-pyridyl)mercury molecules from adjacent layers.

In the structure of compound **6**, the role of uncoordinated ligand molecules is to unite the chains in stair-like arrangements through Hg···π interactions. At supramolecular level, the two types of crystallographically non-equivalent perchlorate anions behave different: perchlorate anions (Cl1) interact with Hg atoms belonging to coordinated organometallic spacers in adjacent double chains, thus assembling two-dimensional supramolecular layers (Hg1···O10^c = 3.029(18) Å; ^{c} = 1-*x*, 1-*y*, -*z*), the other crystallographically independent perchlorate anions (Cl2) connect the layers in a three-dimensional supramolecular network by semi-coordination of oxygen atoms to the mercury(II) atoms from neighboring layers (Hg1 ··· O5^d = 3.081(13) Å; ^{d} = 2-x, 1-y, 1-z).

By replacing the perchlorate anions with the tetrafluoroborate anions, displaying a lower coordination capacity, a three-dimensional coordination polymer was obtained, where bis(4-pyridyl)mercury bridge the $\{Cu_2(pa)_2\}^{2+}$ binuclear nodes in a cationic network, with a topology is similar to the one present in $CdSO_4$ structure (figure 3). The crystal packing diagram of compound **7** contains four interpenetrated independent networks.

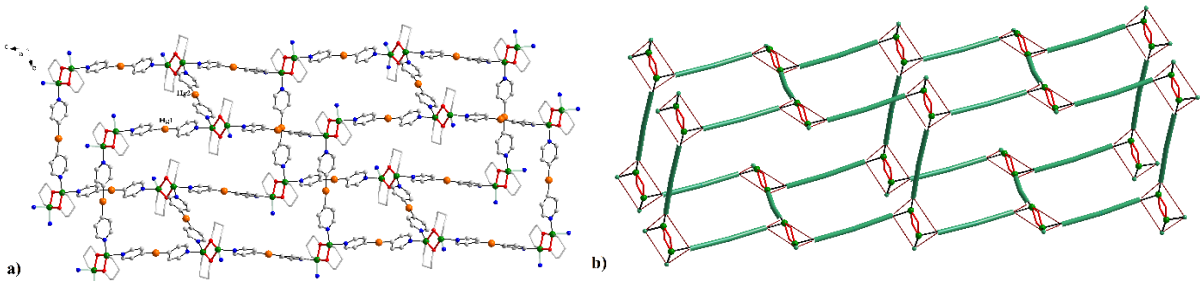

Figure 3. a) Perspective of a three-dimensional network in the structure of compound **7**; b) Representation of the 3-D network with the topology of $CdSO_4$, **cds**, highlighting the orientation of the square-planar $\{Cu_2(pa)_2\}^{2+}$ nodes.

The structural features of bis(4-pyridyl)mercury molecules promote the utilization of the organometallic tectons in generating robust supramolecular synthons by involving the pyridyl groups in hydrogen bonds or the Hg atom in various non-covalent interactions (Hg···O, Hg···N, Hg···π). The dependence on the number and orientation of phenolic groups and acid strength of the nature of the systems resulted by interacting bis(4-pyridyl)mercury and various

molecules, decorated with OH or COOH groups, playing the role of donors in H-bonds formation, was studied (scheme 2).

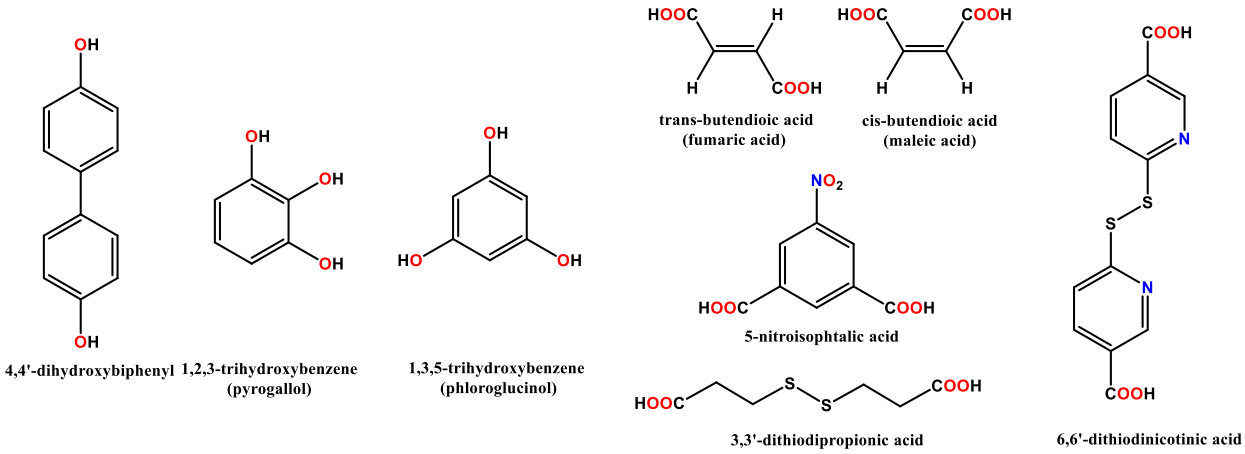

Schema 2. The structures of the phenols and organic acids used in chapter II.

The reaction between bis(4-pyridyl)mercury and phenol tectons led to the formation of co-crystallization products where the two components are organized into supramolecular aggregates by homo- and heterosynthons based on Hg···E (O, N) interactions or hydrogen bonds (N···HO, O···HO). For compounds 4,4'-dihydroxybiphenyl: bis(4-pyridyl)mercury (1: 1) **8** and 1,2,3-trihydroxybenzene: bis(4-pyridyl)mercury (1: 1) **9**, the solid state architecture is modeled by the presence of Hg···O, π–π stacking interactions and N···HO hydrogen bonds, but the structural features of phenolic molecules lead to the assembly of different synthons. In compound **8**, 4,4'-dihydroxybiphenyl and bis (4-pyridyl) mercury form supramolecular chains through hydrogen bonds (N···HO), that are connected in a three-dimensional network by Hg···O contacts (figure 4 a, b). Two such networks interpenetrate, the phenyl and pyridyl fragments belonging to different networks being involved in π–π stacking interactions. In the case of compound **9** is a two-dimensional supramolecular network with herringbone topology, where the center of the phenyl rings and the Hg(II) atoms constitute three connectivity nodes, and is assembled by Hg···O interactions and hydrogen bonds (N···HO) between 1,2,3-trihydroxybenzene and bis(4-pyridyl)mercury. π–π stacking contacts are established between the pyridyl rings arising from two independent layers (centriod-centriod distance is 3.68 Å) – figure 4c.

The reaction between 1,3,5-trihydroxybenzene and bis(4-pyridyl)mercury afforded the formation of compound **10**, having the two tectons in a 1: 2 molar ratio. The crystal structure of **10** is described by a series of supramolecular motifs constructed by assembling homo- and heterosynthons based on hydrogen bonds (N···HO, O···HO) or mercury-interactions (Hg···O,

Hg···N). The supramolecular homomeric chains of phloroglucinol and bis(4-pyridyl)mercury, generated through hydrogen bonds O···HO, Hg···N contacts, respectively, are interconnected in two-dimensional layers by hydrogen bonds between the third OH group of the phenol component and a nitrogen atom belonging to L^1 molecules (Hg1). Hg2 mercury atoms from one layer are involved in Hg···O interactions with phenol groups from neighboring layers, generating a three-dimensional network. The crystal packing diagram illustrates the interpenetration of two 3-D supramolecular networks.

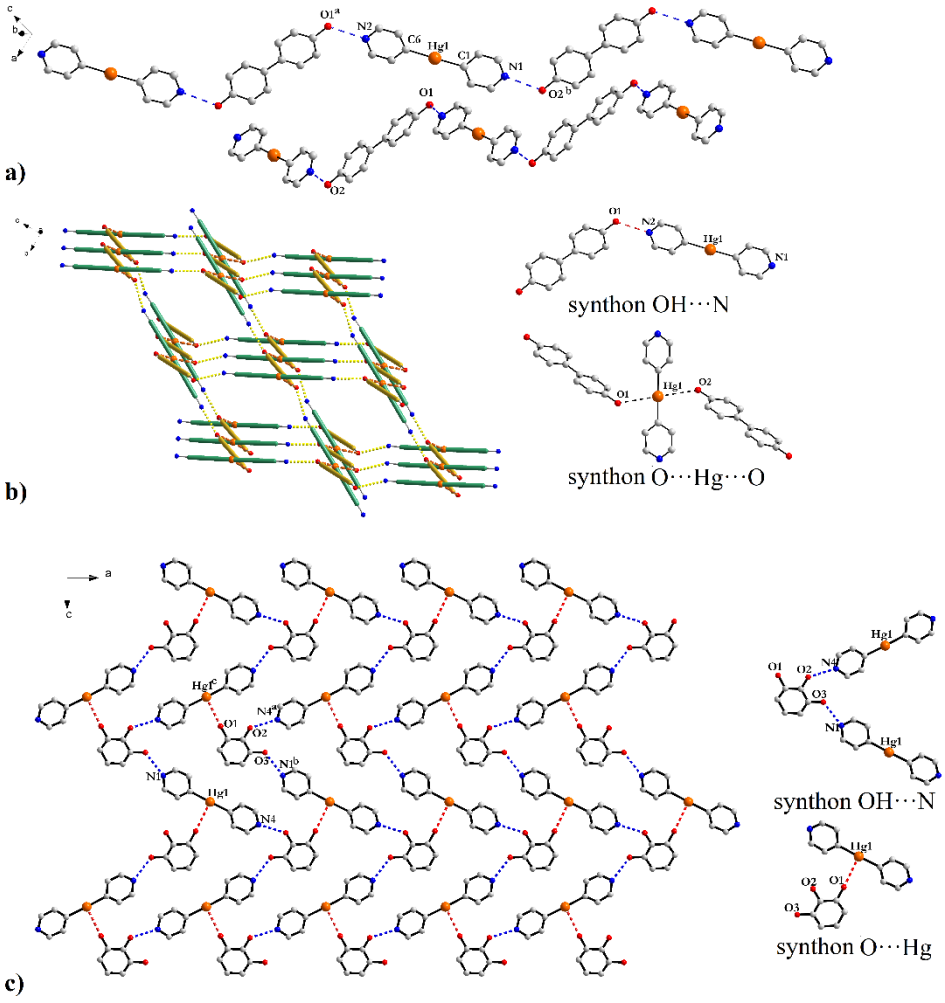

Figure 4. Crystal structure of 8: a) Two supramolecular chains with different orientations constructed by hydrogen bonds between bis(4-pyridyl)mercury and 4,4'-dihydroxybiphenyl; b) 3-D supramolecular network obtained by assembling the OH···N and O···Hg···O heterosynthons. Symmetry operations: [a] = *x*, 1.5-*y*, 0.5+*z*; [b] = -1+*x*, 0.5-*y*, -0.5+*z*. Crystal structure of 9: c) Supramolecular layer with herring bone topology constructed by supramolecular heterosynthons based on hydrogen bonds and Hg···O interactions between pyrogallol and bis(4-pyridyl)mercury molecules. Symmetry operations [a] = -0.5+*x*, 2-*y*, *z*; [b] = *x*, 1+*y*, *z*; [c] = -0.5+*x*, 1-*y*, *z*.

A study on the influence of acid strength on the nature of supramolecular systems was performed using different dicarboxylic acids with various geometries (linear, angular, helical):

trans-butenedioic acid, cis-butenedioic acid, 5-nitroisophthalic acid, 6,6'- dithiodinicotinic acid, 3,3'-dithiodipropionic acid. Hydrated organic salts are assembled in the case of more acidic tectons by propagating the COO···HN synthon at one-dimensional level and associating the chains in three-dimensional supramolecular networks (**11**, **13**) or two-dimensional layers with bi-layer topology (**14**) considering the hydrogen bonds involving lattice water molecules and Hg···O, Hg···N interactions. The reaction of maleic acid with bis(4-pyridyl)mercury yields two types of colorless single crystals: *i*) cubic crystals with the same structure as in compound **11**, where a total isomerization of maleic acid molecules into fumaric acid took place; *ii*) acicular crystals, where only a part of the maleic acid molecules has been transformed into fumaric acid in the structure of compound **12**, which represents a ternary system having diprotonated bis(4-pyridyl)mercury molecules, $Hfum^-$ anions and molecules of maleic acid assembled by hydrogen bonds in a three-dimensional, binodal network with **dmd** topology. Compound **15** exhibits a double-interpenetrated binary three-dimensional network with four connectivity nodes with each tecton involved in Hg···O interactions or COOH···N hydrogen bonds, considering the 3,3'-dithiodipropionic acid being the weakest Brönsted acid from the series of acids used.

Neutral units $\{Mn(hfac)_2\}$ were used as assembling species in order to avoid the transmetallation reactions that trimethylstibium(V)-bi(isonicotinate) may undergo in the presence of perchlorate and nitrate anions. The crystal structure of compound **17** contains linear chains, the trimethylstibium(V)-bi(isonicotinate) L^2 ligand coordinating in the *trans* positions of the metal building blocks.

Bi(V) organometallic derivatives grafted with nicotinate and isonicotinate fragments have been used as exo-bidentate ligands to connect silver(I) ions into heterobimetallic networks. The topology and dimensionality of the obtained systems is influenced by the coordinating ability of anions and the presence supramolecular interactions involving Ag(I) ions or pyridyl fragments. The triflate anion functions as bridges between the centers of Ag(I) generating double chains in the structure of compound **18** and two-dimensional layers in compound **19**, when L^3 and L^4 are used, respectively (figure 5). The low coordinating capacity of the hexafluorostibiate anion allows L^3 molecules to act as a tritopic ligand through nitrogen atoms and an oxygen atom, thus assembling a two-dimensional network displaying a bi-layer topology in the structure of **20**. Orientation of 3-pyridyl fragments in *trans* with respect to the plane formed by the Bi(V) atom and the carboxylate groups induces the connection of metal nodes by L^4 spacer molecules in linear chains in compounds **21** and **22**. At supramolecular level the chains are associated into two-dimensional layers by π–π stacking interactions (**21**) and supramolecular three-dimensional networks by π–π stacking and Ag ··· Ag contacts (**22**).

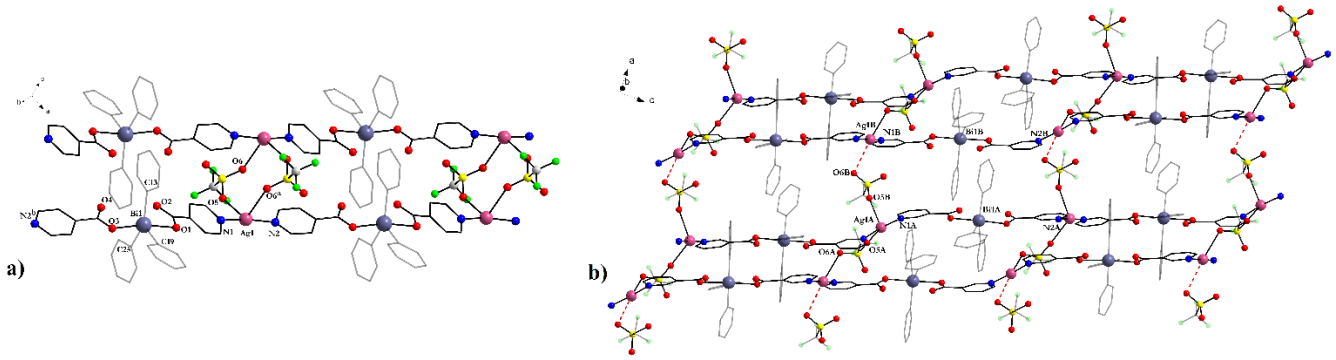

Figure 5. a) Detail of a double chain assembled by triflate bridges in the structure of compound **18**. Symmetry operations: [a] = 1-*x*, 1-*y*, 2-*z*; [b] = -1+*x*, *y*, -1+*z*; b) Perspective of a two-dimensional layer in the structure of compound **19**.

Chapter III presents the synthesis and structural characterization of the coordination polymers obtained by connecting metal ions with spacers exhibiting tetragonal (9,9'-spirobifluorene derivatives) and tetrahedral symmetry (adamantan derivatives and tetra-substituted tin derivative) - scheme 3. Tetragonal ligands are formed by anchoring nitrile groups or pyridyl moieties on 2,2 ', 7,7' positions of 9,9'-spirobifluorene: 9,9′-spirobi[fluorene]-2,2′, 7,7 ′-tetracarbonitrile (L^5) and 2,2′,7,7′-tetrakis(4-pyridyl)-9,9′-spirobi[fluorene] (L^6). Rigid ligands with T_d symmetry used in this chapter constitute derivatives containing nitrile groups and pyridyl fragments arranged on the tetrahedral platform of adamantane: 1,3,5,7-tetrakis{4-(4-pyridyl)phenyl}adamantane (L^7), 1,3,5,7-tetrakis-(4-cyano-phenyl)-adamantan (L^8) or benzoate fragments attached to the tin atom: tetrakis-(4-carboxy-phenyl)-stannane (H_4L^9).

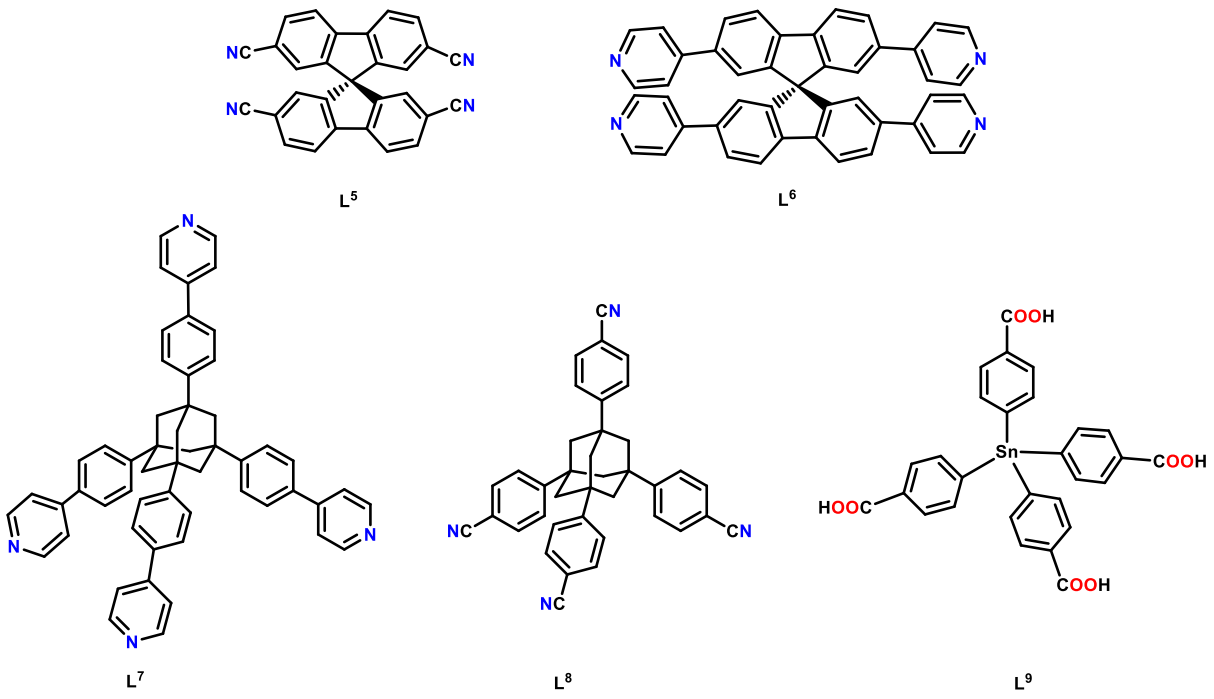

Scheme 3. Organic tectons with tetragonal and tetrahedral geometry used in this thesis.

The structural motifs presented in compounds **23-25** and **27**, obtained from reacting neutral species $\{M(hfac)_2\}$, M^{II} = Cu^{II}, Co^{II}, Mn^{II}, and 9,9'-spirobifluoren derivatives (L^5 and L^6) are imprinted with the orthogonal arrangement of the donor groups in the molecules of the organic ligands and the stereochemical preference of the metal centers. In compounds **23** and **24** (figure 6a) the molecules of 9,9′-spirobi[fluorene] -2,2′,7,7′-tetracarbonitrile (L^5) function as bidentate ligand, connecting the units $\{M(hfac)_2\}$, M^{II} = Cu^{II} (**23**), Co^{II} (**24**), in discrete dinuclear species and linear chains, respectively. Changing the organic ligand : $\{M(hfac)_2\}$ molar ratio from 1: 2 (in **23** and **24**) to 1: 3.15 (**25**) or 1: 4 (**27** – figure 6b) led to the formation of one-dimensional coordination polymers with a double chain topology, where the molecules of L^5 and L^6, respectively, acting as tetradentate bridges, bounded in the *cis* positions of the metal nodes $\{M(hfac)_2\}$.

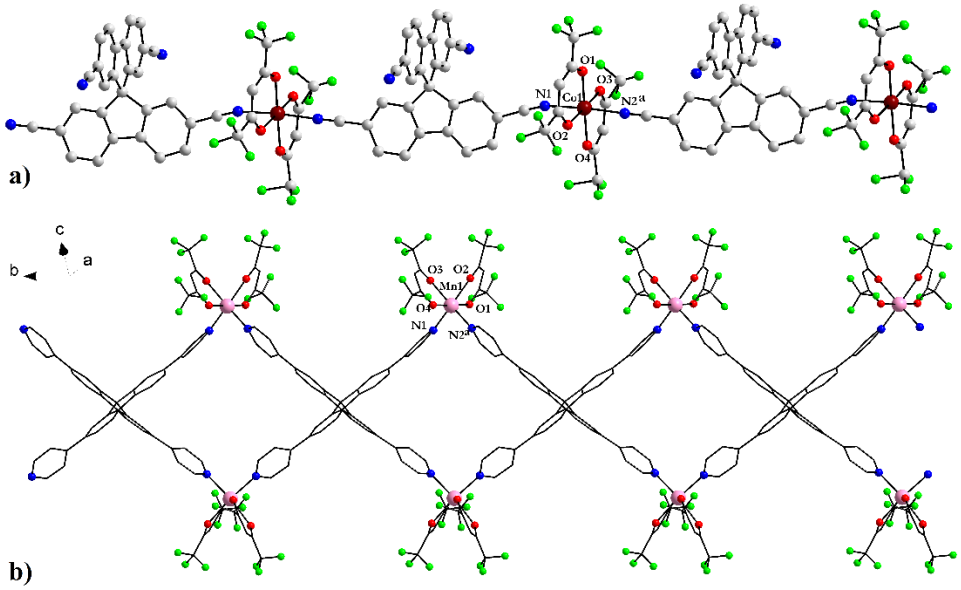

Figure 6. a) View of a one-dimensional chain in the crystal structure of the compound $[Co(hfac)_2L^5]$ **24**. Symmetry operations: [a] = -1+*x*, -1+*y*, *z*; b) Perspective of a double chain in the crystal structure of the compound $[Mn(hfac)_2(L^6)_{0.5}]$ **27**. Symmetry operations: [a] = *x*, -1+*y*, *z*.

Compound $[AgL^5](SbF_6)\cdot CH_3COOC_2H_5$ **26** was constructed by combining the orthogonality of L^5 ligand molecules and the tendency of silver(I) ions to tetracoordinate, and is a two-dimensional coordination polymer with a grid topology, where the metallic centers and spiro carbon atoms represent the four connectivity nodes. The meshes of the **sql** network are alternately occupied by solvent molecules, ethyl acetate, and hexafluorostibiate anions. The single crystals of $[AgL^5](SbF_6)\cdot CH_3COOC_2H_5$ **26** can undergo, by heating at 90˚C, for 48 hours, a *single-crystal-to-single-crystal* process that allows the removal of solvent molecules from the

voids of the network, obtaining thus compound [AgL^5](SbF$_6$) **26a**. The process is reversible, by keeping the crystals of compound **26a** in ethyl acetate vapors the transformation into crystals of **26** takes place (figure 7).

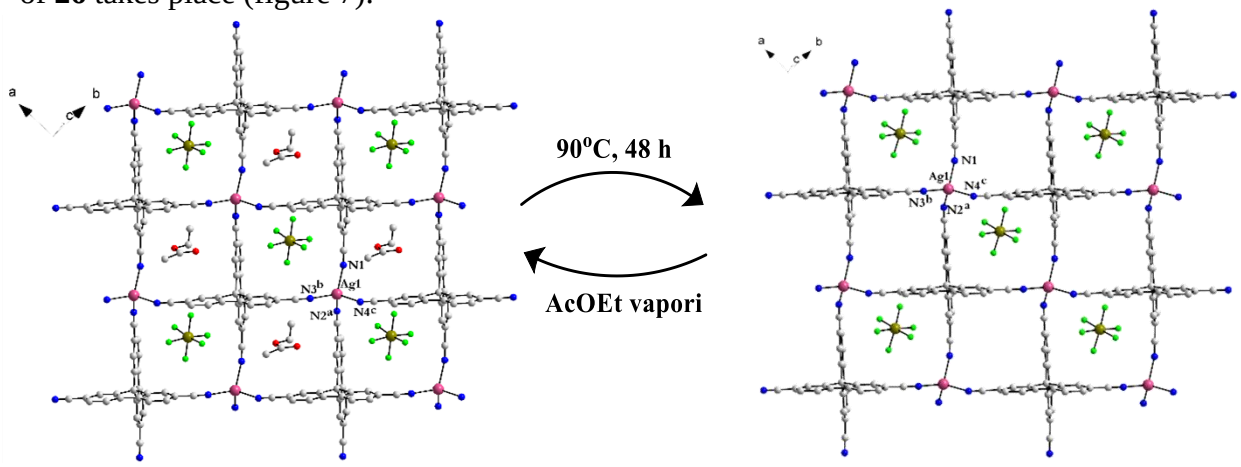

Figure 7. Reversible transformation through a *single-crystal-to-single-crystal* process of [AgL^5](SbF$_6$)·CH$_3$COOC$_2$H$_5$ **26** and [AgL^5](SbF$_6$) **26a** crystals.

The reaction between zinc(II) acetate and 2,2′,7,7′-tetrakis(4-pyridyl)-9,9′-spirobi[fluorene] (L^6) led to the assembly of the one-dimensional coordination polymer [Zn(OAc)$_2$(L^6)$_{0.5}$] **28**, exhibiting double chain structure with similar topology as in **25** and **27**. At the supramolecular level, in compound **27** the adjacent chains are composed either of L^6 molecules with *R* conformation connecting metal centers with octahedral lambda configuration, either from L^6 molecules that adopt *S* conformation and join nodes with delta octahedral configuration, unlike compound **28**, where the pyridyl rings are coplanar with fluorene units, which allows the establishment of contacts π–π stacking between double chains forming a supramolecular layer (figure 8).

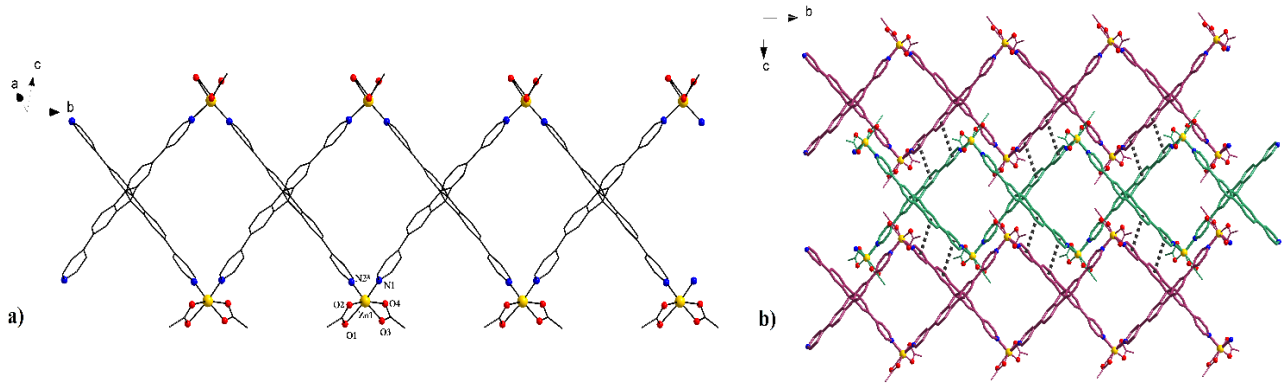

Figure 8. Detail of a double chain in the crystal structure of compound [Zn(OAc)$_2$(L^6)$_{0.5}$] **28**; b) Supramolecular layer built by π – π stacking interactions between double chains with metal centers of different chirality (green - delta, purple - lambda). Symmetry operations: [a] = -*x*, -1+*y*, 0.5-*z*.

Compound **26** emits a blue fluorescence (λ_{em} = 402 nm) when excited with a wavelength of 350 nm, although L^5 molecules do not show luminescent properties, while for compound **28** there is an increase in luminescence intensity and a bathochrome shift of the emission bands compared to the free ligand (from λ_{em} = 425 nm, λ_{ex} = 320 nm for L^6 to λ_{em} = 483 nm, λ_{ex} = 370 nm for **28**), due to more rigid L^6 molecules as a result of coordination to metal ions (figure 9).

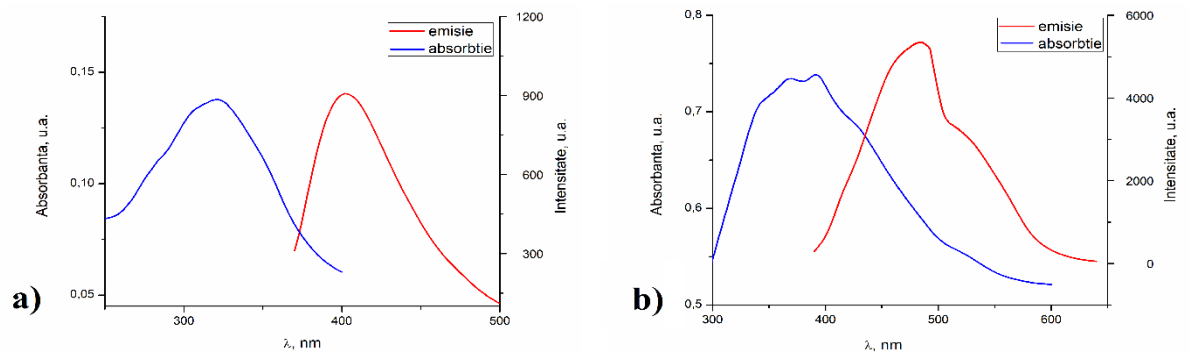

Figure 9. Solid state absorption (blue) and emission (red) spectra of compounds a) $[AgL^5](SbF_6)\cdot CH_3COOC_2H_5$ **26** and b) $[Zn(OAc)_2(L^6)_{0.5}]$ **28**.

L^7 and L^8 ligands, constructed by functionalizing the adamantan core in the 1,3,5,7 positions with donor groups, were used as spacers in the assembling of Cu(II) three-dimensional networks or two-dimensional, grid-like systems, with neutral species $\{M(hfac)_2\}$, M^{II} = Co^{II}, Mn^{II}. The compound $[CuL^7(H_2O)_2](BF_4)_2\cdot 8H_2O$ **29** shows a cationic three-dimensional framework characterized by a PtS topology, where the organic tecton molecules function as a tetrahedral 4-c node, and the metal centers represent the square planar nodes (figure 10a). Although L^8 ligand molecules are tetradentate, and the functionalization of adamantane centers at 1,3,5,7 positions generates an intrinsically three-dimensional orientation of the donor atoms, compounds **30** and **31** are two-dimensional coordination polymers with grid structures, by coordination of L^8 in the *cis* positions of the units $\{M(hfac)_2\}$ (figure 10b).

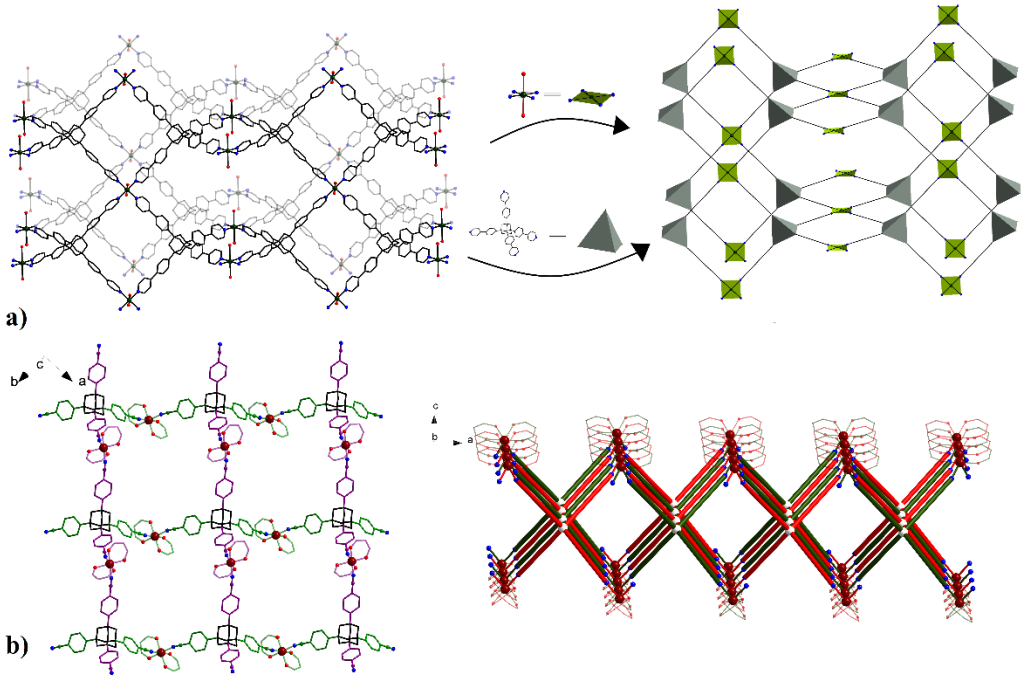

Figure 10. a) Perspective of the cationic network in compound **29** and the representation of the **pts** topology, with the L^7 ligand constituting the tetrahedral nodes and the equatorial plane in the coordination sphere of metal ions - the square planar nodes; b) Perspective of a grid-type layer in the compound **31** and the crystal packing diagram highlighting the 2D→2D interpenetration of two layers and the channels that form in the *ab* plane, seen along the crystallographic *b* axis.

The magnetic properties of compound **31** were investigated (figure 11). The RES spectrum states that the Co(II) ions of compound **31** are characterized by a pseudo-octahedral coordination geometry, an easy-axis magnetic anisotropy, with a high transverse contribution and a low degree of rhombicity ($g_{//}$ = 6.5 and $g_{\perp}$ = 2.6).

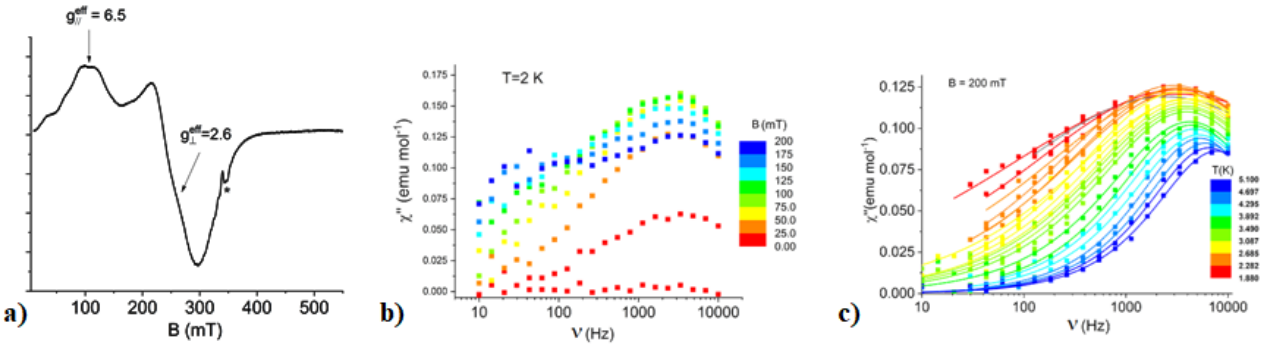

Figure 11. a) EPR spectrum measured for a microcrystalline sample of compound $[Co(hfac)_2(L^8)_{0.5}]$ **31**, at 5 K, (ν = 9.402 GHz); The variation χ" with the frequency for compound **31** measured at: b) 2 K and different values of the magnetic field (0-200 mT); c) 200 mT and different temperatures (1.88-5.10 K). The solid lines represent the fitting of the χ"(ν) curves using a generalized Debey model.

Following the *ac* measurements, the presence of the imaginary component of the magnetic susceptibility is observed only when a magnetic field is applied to suppress the tunneling effect. The variation of the relaxation times vs the temperature suggests that the slow relaxation of the magnetization occurs through several processes, and for the analyzed temperature range, the Raman process is dominant – figure 11 b.

The versatility of the coordination modes that the carboxylate groups can adopt, the arms length and the arrangement of the donor groups in the corners of a tetrahedron are the structural features that recommend the usage of tetrakis-(4-carboxy-phenyl)-stannane (H_4L^9) as a tetratopic spacer in the assembling of neutral three-dimensional networks.

The reaction between a Cu(II) salt and H_4L^9 in the presence of triethylamine and a few drops of ammonia leads to the formation of a three-dimensional coordination polymer $[Cu_2L^9(H_2O)_2]\cdot 3DMF$ **32**. The **pts** topology characterizing the neutral network of compound **32** is described as the connection of the paddle wheel secondary building units, which represent the square planar nodes, and the tin atom representing the tetrahedral nodes. The carboxylate groups coordinate bridging bidentate, joining the metal centers in binuclear clusters. Combining Co(II) ions and H_4L^9, the compound $[Co_2L^9(H_2O)(DMF)_2]\cdot 2DMF\cdot H_2O$ **33** was obtained, where the binuclear units $\{Co_2(COO)_4\}$, showing four extension points describing a distorted tetrahedron, are connected by phenyl rods to Sn tetrahedral nodes, resulting in a neutral three-dimensional framework with diamandoid topology (figure 12). The carboxylate groups in the organic ligand molecule adopt different coordination modes: two COO^- groups act as bridges between two Co (II) ions, the third group joins two metal ions in bridging chelating fashion, while the fourth coordinates bidentate chelating at a single metal center. Two independent **dia** networks interpenetrate.

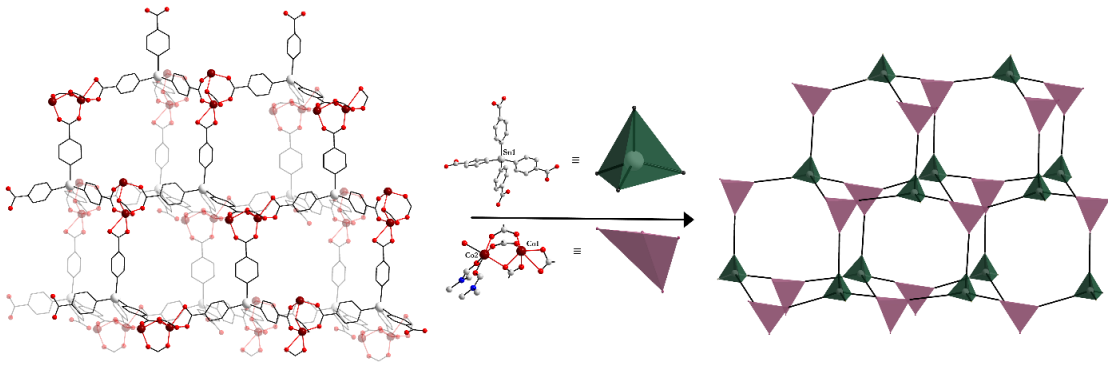

Figure 12. Perspective of the three-dimensional binary network and the schematic representation of the **dia** topology, where the tetrahedral nodes are occupied alternately by the tetradentate organic ligand and the binuclear units $\{Co_2(COO)_4\}$ in compound **33**.

Similarly, diamandoid binary, double interpenetrating networks were assembled by connecting the tetraanion $(L^9)^{4-}$ with tetrahedral metal nodes in which the metal ions display different stereochemistry (tetrahedral (**35**), distorted dodecahedron (**36**), respectively). In compounds $(NH_4)_2[ML^9]$, where M^{II} = Cd^{II} (**35**), Zn^{II} (**36**), the two-interpenetrating anionic diamandoid networks are interconnected by hydrogen bonding of an ammonium cation (figure 13 a,b). In the presence of sodium methoxide and ammonia, the reaction between zinc(II) perchlorate and tetrakis-(4-carboxy-phenyl)-stannane afforded the formation of colorless single crystals of $(NH_4)[NaZnL^9(H_2O)]$ **37**, where the tetrahedral ligand connects Zn(II) and Na(I) ions in a heterotrimetallic anionic network. The four carboxylate groups act as double bridges between Zn(II) and Na(I) ions, grouping the metal centers in one-dimensional structural building units, displaying double-helix structural motifs, and not in discrete SBUs. The three-dimensional anionic network in compound **37** can be described as derived from the structure of compound **36**, by replacing the ammonium cations involved in hydrogen bonds with Na(I) cations, and being composed of two interpenetrated diamandoid networks, where Zn and Sn atoms alternately occupies the tetrahedral nodes. The compound $[NaCo(HL^9)(H_2O)]\cdot H_2O$ **38**, obtained from the reaction between cobalt(II) perchlorate and stananetetrabenzoic acid (H_4L^9), using sodium methoxide as a deprotonator, possesses a neutral heterotrimetallic network, with the topology of the metal centers similar to that of compound **37**, and one of the four arms of the tetrahedral ligand is unprotonated (figure 13 c,d). The reaction between Cd(II) ions and stananetetrabenzoic acid, in the presence of sodium methoxide, as a deprotonating agent, leads to the formation of colorless single crystals of $(NH_4)_{1.5}[Na_{0.5}CdL^9]\cdot 3DMF\cdot H2O$ **39**, where the resulting three-dimensional anionic network shows a fluorine topology, **flu**, with the trinuclear units $\{Cd_2Na(COO)_8\}$ representing eight connected nodes, and the tin center - tetrahedral 4-c nodes.

Although the stanantetrabenzoate tetraanion has a three-dimensional orientation of the carboxylate groups, the blocking with water molecules of *cis* positions in the coordination sphere of Cd(II) ions in the structure of compound $(NH_4)[Cd_{1.5}L^9(H_2O)_2]\cdot 4H_2O$ **34** limits the extension of the lattice in the third dimension. The two-dimensional layers with bi-layer topology of **34** can be described as being composed of adamantan-shaped cages that share eight out of the ten vertices, the other two being occupied by $\{Cd(2)(COO)_2O_2\}$ nodes. Through each layer pass fragments of two other neighboring layers, resulting in a three-dimensional policateneted system (2-D → 3-D).

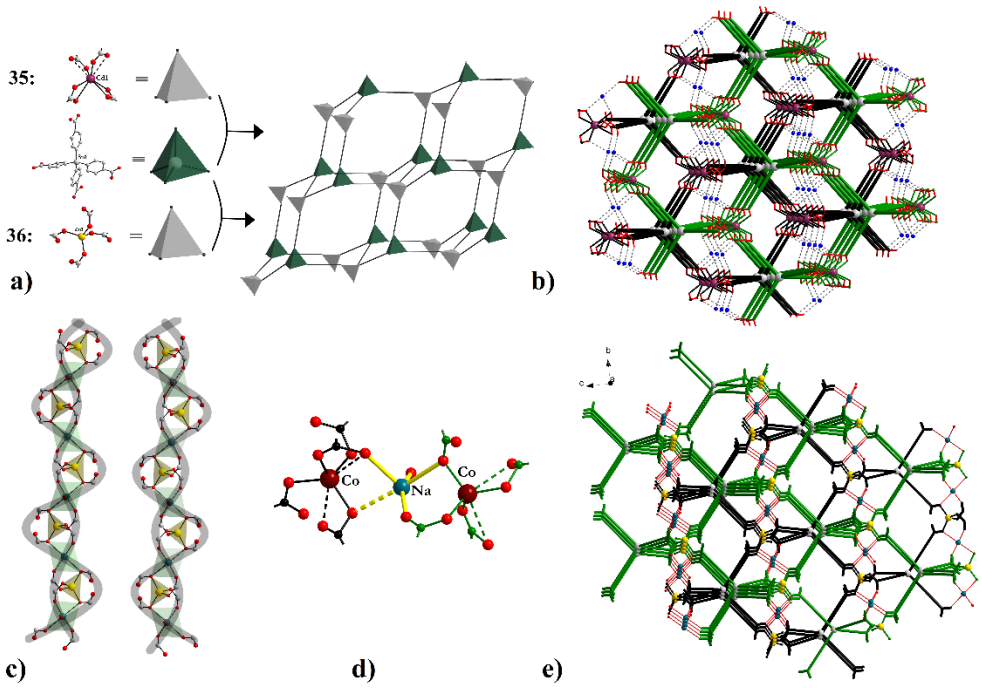

Figure 13. The structure of compounds **35** and **36**: a) Schematic representation of **dia** networks, built with tetrahedral nodes $(L^9)^{4-}$ and $\{Cd(COO)_4\}$, $\{Zn(COO)_4\}$, respectively; b) The crystal packing diagram illustrating two interpenetrated diamandoid networks (green and black) that interact through hydrogen bonds with ammonium cations. Structure of compounds **37** and **38**: c) Two one-dimensional SBUs units of different helicity, assembled by carboxylate bridges and metal ions; d) Connection of two independent **dia** networks with Na(I) ions; e) Crystal packing diagram illustrating two interpenetrated diamandoid networks (green and black) connected by Na(I) cations.

Chapter IV contains the structural description and luminescent properties of coordination compounds built with symmetrical derivatives designed by attaching pyridyl groups to luminescent 2,1,3-benzothiadiazole platforms. The topology and nuclearity of the resulting systems are influenced by a series of factors:

• the geometry of the organic tectons determined by the position of nitrogen atoms in the pyridyl groups that substitute the BTD core. The 4,7-di(2-pyridyl)-2,1,3-benzothiadiazole (2-PyBTD) derivative can adopt several coordination modes and various denticities, while 4,7-di(3-pyridyl)-2,1,3-benzothiadiazole (3-PyBTD) and 4,7-di(4-pyridyl)-2,1,3-benzothiadiazole (4-PyBTD) function as exo-bidentate ligands and can bind metal ions in one-dimensional coordination polymers with different structural motifs;

• the assembling metal species that can direct the final architecture through the position and number of free coordination sites, generating different one-dimensional structural motifs (linear or zig-zag);

• the presence of anions that can act as bridges between metal ions, leading to the assembling of coordination polymers;

• reaction conditions.

The orientation of the pyridyl groups with respect to the benzothiadiazole core plane affords 2-PyBTD molecules the flexibility to present various coordination modes, both pyridine nitrogen atoms and nitrogen atoms in the thiazole fragment can participate in the coordination to cations. The bidentate chelate coordination mode can generate discrete mononuclear units, when the metal centers occupy one of the molecular sites, or binuclear species and coordination polymers when both sites accommodate metal ions. It can also function as a tridentate ligand through the two pyridyl groups and a nitrogen atom in the thiazole ring.

The synthesis of benzothiadiazole derivatives with pyridyl fragments was performed by a Still coupling reaction between 4,7-dibromobenzothiadiazole and (tributylstannyl)pyridine, in the presence of $Pd(PPh_3)$ catalyst 4 (Scheme 4).

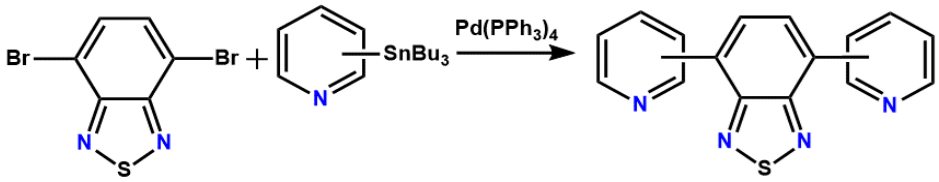

Scheme 4. Synthesis scheme for symmetrical benzothiadiazole derivatives bearing pyridyl fragments.

The series of mononuclear isostructural compounds $[M^{II}(hfac)_2(2\text{-PyBTD})]$, M^{II} = Mn^{II} (**40**), Co^{II} (**41**), Ni^{II} (**42**), Zn^{II} (**43**) – figure 14 a, and dinuclear $[M^{II}_2(hfac)_4(2\text{-PyBTD})]$, M^{II} = Co^{II} (**44**), Ni^{II} (**45**), Zn^{II} (**46**) – figure 15 a, were obtained following the reaction between $\{M(hfac)_2\}$ and 2-PyBTD in a mixture of methanol and chloroform, and dichloromethane and heptane, respectively. The pyridyl groups in the 2-PyBTD molecules show a distinct orientation relative to the benzothiadiazole unit plane in mono- (*cis-trans* conformation) and dinuclear (*cis-cis* conformation) species.

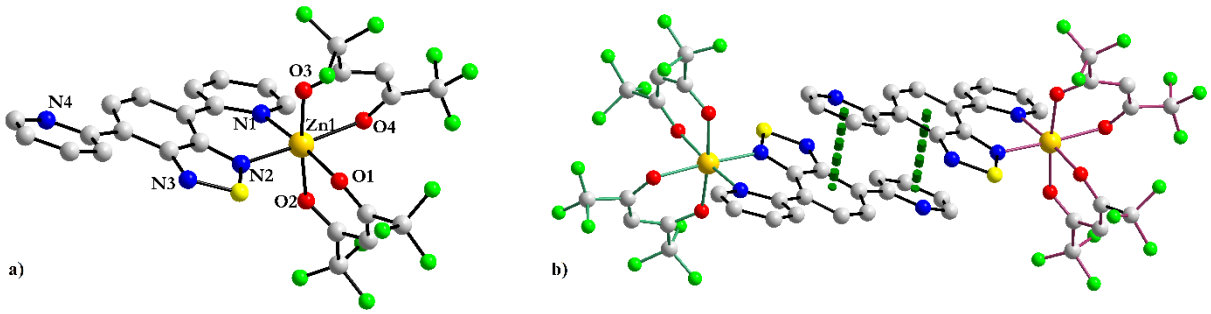

Figure 14. a) The structure of the compound $[Zn(hfac)_2(2\text{-PyBTD})]$ **43**; b) View of a supramolecular dimer built of mononuclear units of different chirality by π – π stacking interactions (green dotted lines) in the structure of compound **43** (green - lambda configuration, purple - delta configuration).

The crystal packing diagram for mononuclear complexes reveals the presence of π–π stacking interactions between phenyl and pyridyl rings from different units with the formation of dimers (figure 14 b). In the case of dinuclear compounds π–π stacking contacts between pyridyl fragments group dinuclear units into supramolecular chains with a *zig-zag* topology (**46**) – figure 15 b, and for compounds **44** and **45**, interactions between pyridyl groups and phenyl rings associate dinuclear species in supramolecular stair-like arrangements.

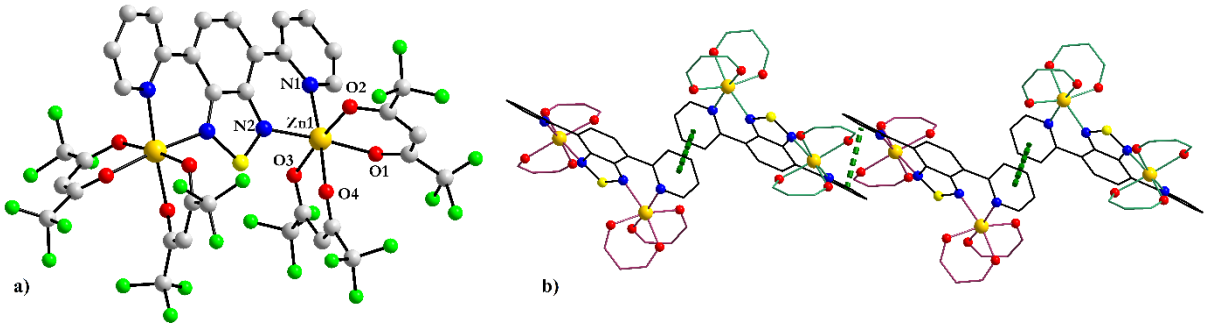

Figure 15. a) The crystal structure of compound $[Zn_2(hfac)_4(2\text{-PyBTD})]$ **46**; b) The crystal packing diagram for compound **46**, illustrating the different chirality of metal centers from neighboring dinuclear units (green - lambda configuration, purple - delta configuration; CF_3 groups were omitted for clarity).

Structural motifs similar to supramolecular stairs in compounds **44** and **45** were obtained by the reacting 2-PyBTD with silver(I) salts ($AgCF_3SO_3$ - **47**, $AgSbF_6$ - **48**). Starting from silver nitrate(I) and 2-PyBTD a two-dimensional coordination polymer, $[Ag_2(NO_3)_2(2\text{-PyBTD})(CH_3CN)]$ **49** was assembled, with the silver ions(I) connected in chains by nitrate anions, which act as μ_4 bridges, and the chains joined in layers by 2-PyBTD molecules, which adopt a *cis-trans* conformation and function as a tridentate ligand. In the compound $[Cu(2\text{-PyBTD})_{0.5}Cl_2]$ **50**, 2-PyBTD molecules are found in a *cis-cis* orientation, and the chloride bridges lead to the formation of a 1-D chain with a wavy structural motif. The different arrangement of nitrogen atoms in the pyridyl fragments of the organic spacers (3-PyBTD and 4-PyBTD) and the coordination of the ligands in either *cis* or *trans* positions of the coordination sphere of $\{Zn(hfac)_2\}$ units generated one-dimensional molecular assemblies with distinct metal centers topology: wavy chains in $[Zn(hfac)_2(3\text{-PyBTD})]$ **51**, figure 16 a, and linear chains in $[Zn(hfac)_2(4\text{-PyBTD})]$ **52**, figure 16b.

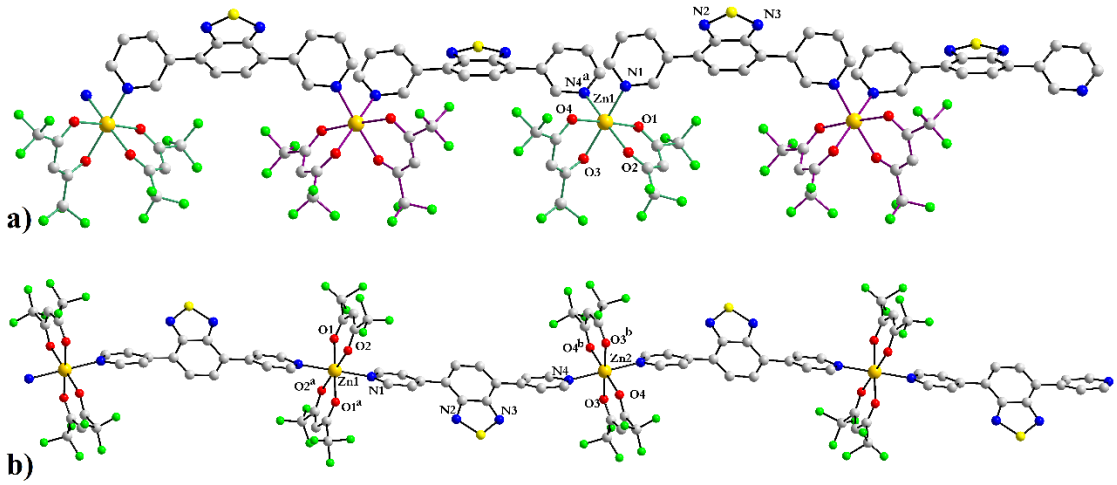

Figure 16. a) Detail of a chain built of {Zn(hfac)$_2$} nodes and 4,7-di (3-pyridyl) -2,1,3-benzothiadiazole molecules in the crystal structure of compound **51**, illustrating the different chirality of neighboring metal centers (green - lambda configuration, purple - delta configuration); b) View of a linear chain in the crystal structure of compound **52**. Symmetry operations [a] = -*x*, 2-*y*, 2-*z*; [b] = 2-*x*, -*y*, 1-*z*.

Compounds [$ZnCl_2$(4-PyBTD)] **53**, figure 17a, and [$ZnCl_2$(4-PyBTD)$_2$] **54**, figure 17b, were obtained starting from $ZnCl_2$ and 4-PyBTD using the same molar ratio, but under different reaction conditions. In the structure of compound **53**, 4-PyBTD molecules function as a bridge ligand, connecting metal ions in *zig-zag* chains, and in compound **54** the benzothiadiazole derivative coordinates to $ZnCl_2$ as a terminal ligand. The π–π stacking interactions associate one-dimensional and mononuclear structures, respectively in 2-D supramolecular layers.

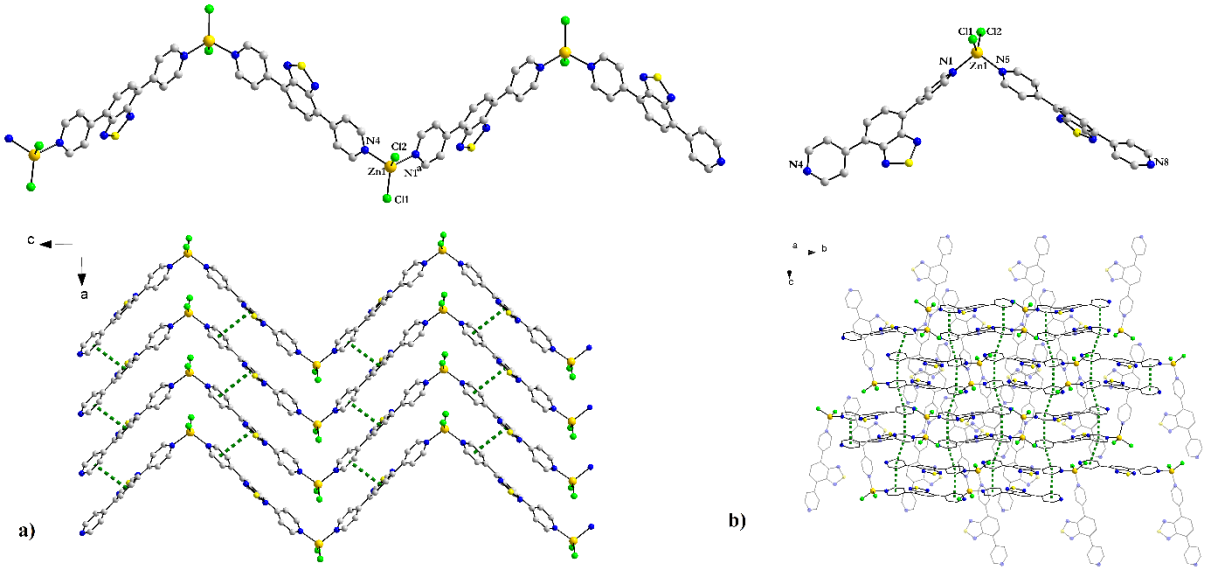

Figure 17. a) Detail of a zig-zag chain in compound **53** and supramolecular layer assembled by associating chains through π – π stacking interactions (green dotted lines). Symmetry operations [a] = 1.5-*x*, 1-*y*, 0.5+*z*. b) Molecular structure of the compound [$ZnCl_2$(4-PyBTD)$_2$] **54** and perspective of two-dimensional layers constructed by π – π stacking contacts (green dotted lines) between pyridyl rings of adjacent mononuclear species.

The photoluminescent properties of 2-PyBTD and 4-PyBTD ligands and compounds constructed with Zn(II) ions, **43**, **46**, **52-54** were studied comparatively. The wavelength values for the absorbed and emissive radiation in the solid state, presented in tables 1 and 2, revealed that in the solid state, following the coordination of benzothiadiazole derivatives to zinc(II) ions, luminescence intensity increases. The observed differences between the emissive properties for compounds **43** and **46** and the free ligand were attributed to the different conformations the ligand molecules adopt (*trans-trans* in the case of the free ligand, *cis-trans* in **43** and *cis-cis* in **46**) and crystal packing of different supramolecular assemblies by π–π stacking interactions - figure 18. The bathochrome shift of the emission bands in solid state compared to those obtained for 2-PyBTD, **43** and **46** in CH_2Cl_2 solution has been attributed to non-covalent interactions that shape the packaging of crystal structures.

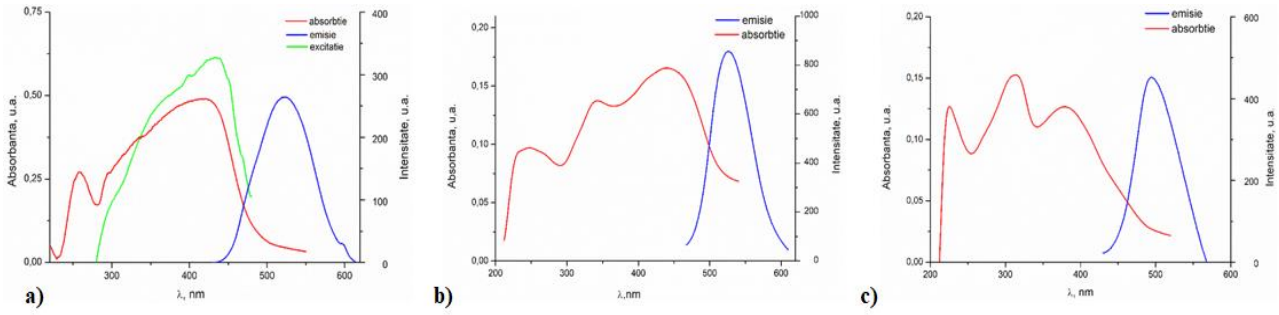

Figure 18. Solid state UV-Vis absorption (red), emission (blue) and excitation (green) for: a) 2-PyBTD ligand; b) compound **43** and c) compound **46**.

Table 1. Photoluminescent properties and structural features for 2-PyBTD and compounds **43** and **46**

	2-PyBTD	**43**	**46**
solid state absorption (nm)	258, 420	247, 343, 440	226, 313, 379
solid state emission (nm)	λ_{ex} = 400, λ_{em} = 523	λ_{ex} = 440, λ_{em} = 526	λ_{ex} = 380, λ_{em} = 495
CH_2Cl_2 solution absorption (nm)	236, 290, 382	265, 314, 381	272, 321, 387
CH_2Cl_2 solution emission (nm)	λ_{ex} = 380, λ_{em} = 466	λ_{ex} = 390, λ_{em} = 467	λ_{ex} = 390, λ_{em} = 470
conformation	*trans-trans*[8]	*cis-trans*	*cis-cis*
Py-BTD dihedral angle (˚)	26.4; 39.1[8]	14.1; 15.3	±26.9
Py-Py dihedral angle (˚)	17.2[8]	7.3	52.9

The nature of the electronic transitions was investigated by DFT and TD-DFT calculations. In the case of compounds **43** and **46**, the HOMO orbitals are located mainly on

the phenyl and pyridyl rings, and the LUMO orbitals are delocalized on the BTD units (figure 19).

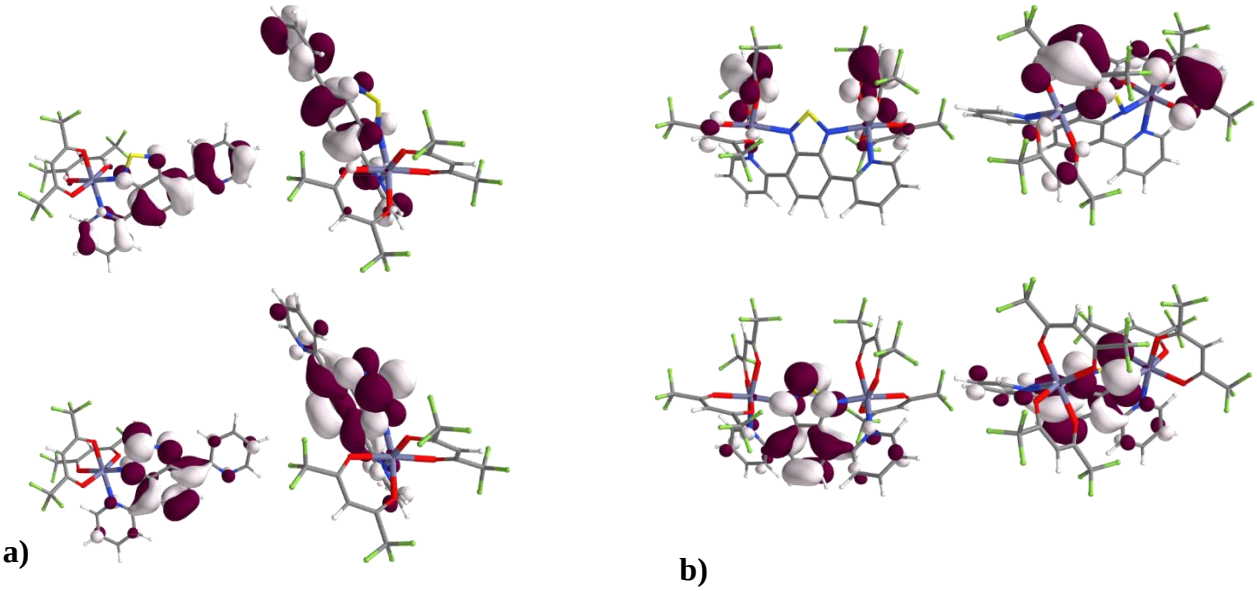

Figure 19. HOMO (top) and LUMO (bottom) orbitals for compounds a) **43**; b) **46**.

The calculated values for the simulated UV-Vis (**43** and **46**) and emission (**43**) spectra (figure 20) are consistent with those observed for the spectra recorded in solution, highlighting the importance of supramolecular interactions that dictate the three-dimensional solid-state assembly of mono- and dinuclear structures.

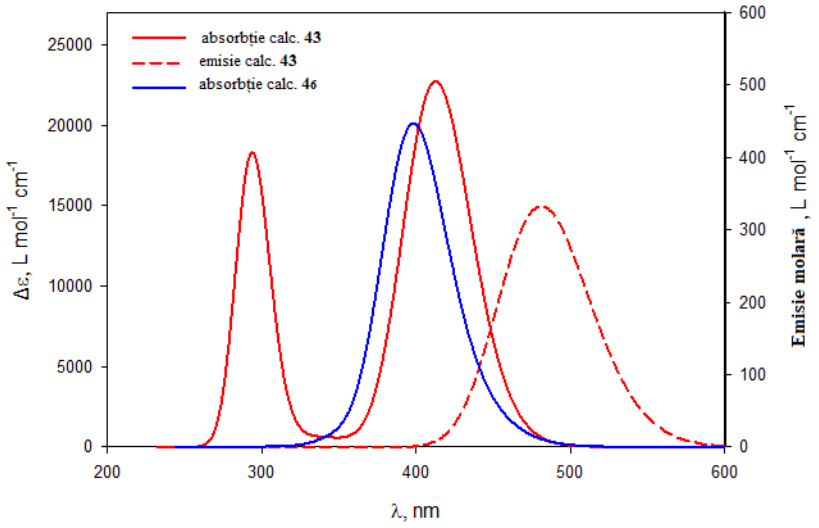

Figure 20. Calculated UV-Vis absorption (solid lines) and emission (dashed lines) spectra for compounds **43** (red) and **46** (blue), characterized by a gaussian distribution (FWHM = 3000 cm^{-1}, TD-DFT/PBE1PBE/TZVP).

In the case of zinc(II) compounds built with the 4-PyBTD spacer, **52-54**, different molecular orbitals involved in electronic transitions (hfac-anions have an attractive electronic

effect, while chloride anions have a π-donor effect) and the presence of supramolecular interactions for compounds **53** and **54** may justify the bathochrome shift of the emission bands following the coordination of organic ligand molecules at the {Zn(hfac)$_2$} nodes in compound **52**, while complexes **53** and **54** show a blue luminescence, similar to that of the 4-PyBTD ligand (figure 21).

Tabel 2. Photoluminescent properties for ligand 4-PyBTD and compounds **52-54**

	absorption (nm)	emission (nm)
4-PyBTD	260, 397	λ_{ex} = 370, λ_{em} = 472
52	335, 385	λ_{ex} = 460, λ_{em} = 527
53	254, 411	λ_{ex} = 400, λ_{em} = 471
54	270, 348	λ_{ex} = 410, λ_{em} = 476

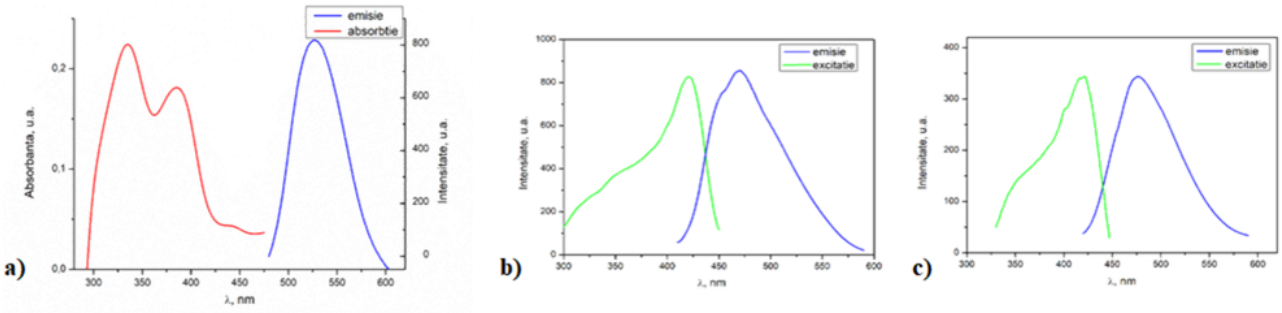

Figure 21. Solid state UV-Vis absorption (red), emission (blue) and excitation (green) spectra for compounds: a) **52**; b) **53** and c) **54**.

Within the present PhD thesis, 54 new compounds were synthesized and characterized by single crystal X-ray diffraction spectroscopic measurements. Photoluminescence studies were performed for 7 compounds, and one compound is magnetically characterized. The results obtained demonstrate the effectiveness of organometallic molecules as tectons in supramolecular chemistry and crystalline engineering, the topological diversity generated by the use of tetragonal and tetrahedral shaped spacers and the vast chemistry built with multifunctional ligands derived from benzothiadiazole.

Selected references:

CHAPTER I

8. a) O. M. Yaghi, Hailian Li, J *Am. Chem. Soc.*, **1995**, *117*, 10401; b) O. M. Yaghi, G. Li, H. Li, *Nature*, **1995**, *378*, 703.
9. S. R. Batten, N. R. Champness, X.-M. Chen, J. Garcia-Martinez, S. Kitagawa, L. Öhrström, M. O'Keeffe, M. Paik Suh, J. Reedijk, *Pure Appl. Chem*., **2013**, *85*, 1715.
10. N. Connelly, T. Damhus, R. M. Harshorn, IUPAC. *Nomenclature of Inorganic Chemistry, IUPAC Recommendations 2005* (the "Red Book"), RSC Publishing, Cambridge, UK, **2005**.
11. O. M. Yaghi, M. J. Kalmutzki, C. S. Diercks, Introduction to Reticular Chemistry Metal–Organic Frameworks and Covalent Organic Frameworks, Wiley-VCH, Weinheim, **2019**, p. 431-452.
12. O. Delgado-Friedrichs, M. O'Keeffe, *J. Solid State Chem*., **2005**, *178*, 2480.
13. a) A. F. Wells, Three-Dimensional Nets and Polyhedra; John Wiley & Sons: New York, **1977**; b) A. F. Wells, Further Studies of Three-Dimensional Nets; Monograph 9; Am. Cryst. Assoc.: Littleton, CO, **1979**.
23. L. Öhrström, K. Larsson, *Molecule-Based Materials: The Structural Network Approach*; Elsevier: Amsterdam, The Netherlands, **2005**, p. 42.
24. S. R. Batten, S. M. Neville, D. R. Turner, *Coordination Polymers: Design, Analysis and Application*; Royal Society of Chemistry: Cambridge, **2009**.
34. O. Delgado-Friedrichs, M. D. Foster, M. O'Keeffe, D. M. Proserpio, M. M. J. Treacy, O. M. Yaghi, *J. Solid State Chem*., **2005**, *178*, 2533.
35. V.A. Blatov, L. Carlucci, G. Ciani, D.M. Proserpio, *Cryst. Eng. Comm*., **2004**, *6*, 377.
36. O. Delgado-Friedrichs, M. O'Keeffe, O.M. Yaghi, *Solid State Sci*., **2003**, *5*, 73.
62. R. Robson, *Dalton Trans*., **2008**, 5113.
63. B. F. Abrahams, S. R. Batten, H. Hamit, B. F. Hoskins, R. Robson, *Chem. Commun*., **1996**, 1313.
64. B. F. Abrahams, S. R. Batten, M. J. Grannas, H. Hamit, B. F. Hoskins, R. Robson, *Angew. Chem. Int. Ed*., **1999**, *38*, 1475
65. B. F. Abrahams, S. R. Batten, H. Hamit, B. F. Hoskins, R. Robson, *Angew. Chem., Int. Ed. Engl*., **1996**, *35*, 1690.
66. a) H. W. Roesky, M. Andruh, *Coord. Chem. Rev*., **2003**, *236*, 91; b) M. J. Zaworotko, *Cryst. Growth Des*., **2007**, *7*, 4; c) K. Biradha, M. Sarkar, L. Rajput, *Chem. Commun*., **2006**, 4169.

CHAPTER II

2. a) M. Andruh, *Pure Appl. Chem*., **2005**, *77*, 1685; b) M. Andruh, *Chimia*, **2013**, *67*, 383; c) M. Andruh, *Chem. Commun.*, **2007**, 2565; d) J. K. Clegg, F. Li, L. F. Lindoy, *Coord. Chem. Rev*., **2013**, *257*, 2536; e) S. Biswas, C. J. Gomez-García, J. M. Clemente-Juan, S. Benmansour, A. Ghosh, *Inorg. Chem*., **2014**, *53*, 2441.
19. a) D. Braga, L. Maini, M. Polito, M. Rossini, F. Grepioni, *Chem. Eur. J*., **2000**, *6*, 4227; b) D. Braga, L. Maini, M. Polito, F. Grepioni, *Chem. Commun*., **2002**, 2302; c) D. Braga, L. Maini, S. L. Giaffreda, F. Grepioni, M. R. Chierotti, R. Gobetto, *Chem. Eur. J*., **2004**, *10*, 3261.
35. I. Haiduc, F.T. Edelmann, *Supramolecular Organometallic Chemistry*, Wiley, Weinheim, **2007**.

36. a) C. G. dos Santos, G. M. de Lima, *Coord. Chem. Rev*., **2020**, *410*, 213236*;* b) M. M. Amini, E. Najafi, H. Saeidian, E. Muhammadi, S.M. Shahabi, S.W. Ng, *Appl. Organomet. Chem.*, **2017**, *31*, e3884; c) A. E. Ghionoiu, D.-L. Popescu, C. Maxim, A. M. Madalan, I. Haiduc, M. Andruh, *Inorg. Chem. Commun*., **2015**, *58*, 71; d) C. Ma, Y. Han, R. Zhang, D. Wang, *Eur. J. Inorg. Chem.*, **2005**, 3024.

43. a) D. Braga, F. Grepioni, G. R. Desiraju, *Chem. Rev*., **1998**, *98*, 1375; b) G. R. Desiraju, *J. Chem. Soc., Dalton Trans.*, **2000**, 3745; c) K. Biradha, C.-Y. Su, J. J. Vittal, *Cryst. Growth Des.*, **2011**, *11*, 875

47. a) M. Tsunoda, F. P. Gabbï, *J. Am. Chem. Soc.*, **2000**, *122*, 8335; b) K. I. Tugashov, D. A. Gribanyov, F. M. Dolgushin, A. F. Smol'yakov, A. S. Peregudov, Z. S. Klemenkova, I. G. Barakovskaya, I. A. Tikhonova, V. B. Shur, *Organometallics*, **2019,** *38*, 2910; c) M. R. Haneline, F. P. Gabbï, *Inorg. Chem*., **2005**, *44*, 6248.

64. a). V. Tudor, G. Marin, V. Kravtsov, Y. A. Simonov, J. Lipkowski, M. Brezeanu, M. Andruh, *Inorg. Chim. Acta*, **2003**, *353*, 35; b) G. Marin, V. Tudor, V. Ch. Kravtsov, M. Schmidtmann, Y. A. Simonov, A. Müller, M. Andruh, *Cryst. Growth Des.*, **2005**, *5*, 279; c) G. Marin, V. Kravtsov, Y. A. Simonov, V. Tudor, J. Lipkowski, M. Andruh, *J. Molec. Struct.*, **2006**, *796*, 123; d) G. Marin, M. Andruh, A. M. Madalan, A. J. Blake, C. Wilson, N. R. Champness, M. Schröder, *Cryst. Growth Des.*, **2008**, *8*, 964.

85. C. B. Aakeröy, M. E. Fasulo, John Desper, *Mol. Pharmaceutics*, **2007**, *4*, 317.

86. a) M. C. Etter, *Acc. Chem. Res*., **1990**, *23*, 120; b) M. C. Etter, G. M. Frankenbach, *Chem. Mater*., **1989**, *1*, 10; c) M. C. Etter, *J. Phys. Chem*., **1991**, *95*, 4601.

87. a) G. R. Desiraju, *Angew. Chem., Int. Ed. Engl.*, **1995**, *34*, 2311; b) G. R. Desiraju, *Chem Commun*., **1997**, 1475; c) J. A. R. P. Sarma, G. R. Desiraju, *Cryst. Growth Des*., **2002**, *2*, 93.

88. a) C. B. Aakeröy, A. M. Beatty, B. A. Helfrich, *Angew. Chem., Int. Ed*., **2001**, *40*, 3240; b) C. B. Aakeröy, J. Desper, M. M. Smith, *Chem. Commun*., **2007**, 3936.

89. M C Etter, J C MacDonald, J Bernstein, *Acta Cryst. Sect B*, **1990**, *46*, 256.

CHAPTER III

34. T. Muller, S. Bräse, *RSC Adv*., **2014**, *4*, 6886.

37. R. Boča, *Coord. Chem. Rev*., **2004**, *248*, 757; b) J. Titiš, R. Boča, *Inorg. Chem*., **2011**, *50*, 11838.

47. D. J. Tranchemontagne, J. L. Mendoza-Cortés, M. O'Keeffe, O. M. Yaghi, *Chem. Soc. Rev*., **2009**, *38*, 1257.

48. a) O. M. Yaghi, M. O'Keeffe, N. W. Ockwig, H. K. Chae, M. Eddaoudi, J. Kim, *Nature*, **2003**, *423*, 705; b) O. M. Yaghi, *Mol. Front. J*., **2019**, *3*, 66.

CHAPTER IV

1. a) T. Hirao, *Coord. Chem. Rev*., **2002**, *226*, 81; b) L. Pu, *Chem. Rev*., **2004**, *104*, 1687; c) S. S. Sun, A. J. Lees, *J. Am. Chem. Soc.*, **2000**, *122*, 8956; d) C. D. Dimitrakopouls, P. R. L. Malenfant, *Adv. Mater*., **2002**, *14*, 99; e) Y. Sun, Y. Liu, D. Zhu, *J. Mater. Chem.*, **2005**, *15*, 53; f) B. Xu, X. Xiao, X. Yang, L. Zang, N. Tao, *J. Am. Chem. Soc.*, **2005**, *127*, 2386; g) C. R. Newman, C. D. Frisbie, D. A. da Silva Filho, J.-L. Brédas, P. C. Ewbank, K. R.Mann, *Chem. Mater*., **2004**, *16*, 4436.
2. a) B. A. D. Neto, A. A. M. Lapis, E. N. da Silva Júnior, J. Dupont, *Eur. J. Org. Chem.*, **2013**, 228; b) B. A. D. Neto, P. H. P. R. Carvalho, J. R. Correa, *Acc. Chem. Res*., **2015**, *48*, 1560; c) A. A. R. Mota, J. R. Correa, P.

H. P. R. Carvalho, N. M. P. de Sousa, H. C. B. de Oliveira, C. C Gatto, D. A. da Silva Filho, A. Lima de Oliveira, B. A. D. Neto, *J. Org. Chem.*, **2016**, *81*, 2958; d) B. A. D. Neto, A. S.'A. Lopes, G. Ebeling, R. S. Gonçalves, V. E. U. Costa, F. H. Quina, J. Dupont, *Tetrahedron*, **2005**, *61*, 10975.

8. Md. Akhtaruzzaman, M. Tomura, J. Nishida, Y. Yamashita, *J. Org. Chem*., **2004**, *69*, 2953.

I. List of published articles in the PhD thesis field

1. *Bis-(4-pyridyl)mercury – a new linear tecton in crystal engineering: coordination polymers and co-crystallization processes*, **T. Mocanu**, C. I. Raţ, C. Maxim, S. Shova, V. Tudor, C. Silvestru, M. Andruh, *CrystEngComm*, **2015**, *17*, 5474.
2. *Coordination polymers constructed from tetrahedral-shaped adamantane tectons*, **T. Mocanu**, L. Pop, N. D. Hădade, S. Shova, I. Grosu, M. Andruh, *CrystEngComm*, **2017**, *19*, 27.
3. *Alkoxido-bridged binuclear copper(II) complexes derived from aminoalcohols – useful building blocks in designing coordination polymers with a rich structural variety*, **T. Mocanu**, V. Tudor, M. Andruh, *CrystEngComm*, **2017**, *19*, 3538.
4. *Triphenylbismuth(V) di[(iso)nicotinates] – transmetallation agents or divergent organometalloligands? First organobismuth(V)-based silver(I) coordination polymers*, A. Ben Kiran, **T. Mocanu**, A. Pollnitz, S. Shova, C. Silvestru, M. Andruh, *Dalton Trans.*, **2018**, *47*, 2531.
5. *Coordination polymers and supramolecular solid-state architectures constructed from an organometallic tecton, bis(4-pyridyl)mercury*, **T. Mocanu**, L. Kiss, A. Sava, S. Shova, C. Silvestru, M. Andruh, *Polyhedron*, **2019**, *166*, 7.
6. *Structural Diversity Ranging from Oligonuclear Complexes to 1-D and 2-D Coordination Polymers Generated by Tetrasubstituted Adamantane and Spirobifluorene Derivatives*, **T. Mocanu**, L. Pop, N. D. Hădade, S. Shova, L. Sorace, I. Grosu, M. Andruh, *Eur. J. Inorg. Chem.*, **2019**, 5025.
7. *Dimensionality Control in Crystalline Zinc(II) and Silver(I) Complexes with Ditopic Benzothiadiazole-Dipyridine Ligands*, **T. Mocanu**, N. Plyuta, T. Cauchy, M. Andruh, N. Avarvari, *Chemistry*, **2021**, *3*, 269.

II. Other published articles during the Ph.D thesis

1. *New mixed-valence disk-like [Co7] clusters with aminoalcohol ligands*, A. A. Apostol, G. Vasile, **T. Mocanu**, C. Maxim, V. Tudor, M. Andruh, *Rev. Roum.Chim.*, **2020**, *65*, 711.

2. *Luminescent [ZnIIEuIII] and [ZnIITbIII] complexes anchored on graphene*, A. A. Apostol, I. Mihalache, **T. Mocanu**, O. Tutunaru, C. Pachiu, R. Gavrila, C. Maxim, M. Andruh, *Appl Organomet Chem.*, **2021**, *35*, e6126.

3. *Magnetic molecular rectangles constructed from functionalized nitronyl-nitroxide ligands and lanthanide(III) ions*, S. Calancea, L. Carrella, **T. Mocanu**, V. Sadohin, M. Raduca, I. Gutu, J. C. da Rocha M. G. F. Vaz, E. Rentschler, M. Andruh, *Eur. J. Inorg. Chem.*, **2021**, 567.

4. *Synthesis, crystal structure, magnetic, spectroscopic, and theoretical investigations of two new nitronyl-nitroxide complexes*, C. A. Spinu, C. Pichon, G. Ionita, **T. Mocanu**, S. Calancea, M. Raduca, J.-P. Sutter, M. Hillebrand, M. Andruh, *J. Coord. Chem.*, **2021**, doi: 10.1080/00958972.2021.1871900.

III. List of scientific communications:

1. „*Coordination polymers of various dimensionalities built with tetradentate spacers*"; **T. Mocanu**, S. Shova, C. Silvestru, I. Grosu, M. Andruh. **National Conference of Doctoral Schools form Universitaria Consortium, 31 October-03 November 2018, Iași, Romania,** oral presentation.
2. „*Coordination polymers of various topologies built from tetradentate spacers*"; **T. Mocanu**, S. Shova, C. Silvestru, I. Grosu, M. Andruh. **XXXV-th National Conference on Chemistry, 02-05 October 2018, Călimănești – Căciulata, Romania**, oral presentation.
3. „*Organometallic and tetrahedral spacers – new tectons in crystal engineering and metallosupramolecular chemistry*", **T. Mocanu**, M. Andruh. **Workshop: Crystal-engineering of multifunctional molecule based-materials, 3-6 May 2016, Sinaia, Romania**, oral presentation.
4. „*Coordination polymers built with oligonuclear nodes*", **T. Mocanu**, C. Maxim, C. Silvestru, M. Andruh. **Anniversary Symposium "Faculty of Chemistry – 150 years of traditions" – Session of Doctoral School in Chemistry, Bucharest, 14 June 2014**, oral presentation.
5. *„Bis(4-pyridyl)mercury – a new linear tecton in crystal engineering: coordination polymers and co-crystallization processes"*, **T. Mocanu**, C. I. Raţ, C. Maxim, S. Shova, V. Tudor, C. Silvestru, M. Andruh. **10th International Symposium on Macrocyclic and Supramolecular Chemistry, 28 June-2 Julie 2015, Strasbourg, France**, poster.

6. „*Divergent organometallic spacers as tectons in coordination polymers and supramolecular architectures”*, **T. Mocanu**, S. Shova, C. Silvestru, M. Andruh. **Student Scientific Communication Session, 25-26 May, 2018, Faculty of Chemistry, Bucharest**, oral presentation.
7. „*Coordination polymers of various topologies constructed from tetradentate spacers*”, **T. Mocanu**, S. Shova, C. Silvestru, I. Grosu, M. Andruh. **Student Scientific Communication Session, 26 May, 2017, Faculty of Chemistry, Bucharest**, oral presentation.
8. *„Organometallic and tetrahedral spacers – new tectons in crystal engineering and metallosupramolecular chemistry”*, **T. Mocanu**, C. Maxim, C. Silvestru, I. Grosu, M. Andruh. **Student Scientific Communication Session, 20 May, 2016, Faculty of Chemistry, Bucharest**, oral presentation.